ELASTO-PLASTIC BEHAVIOR OF STEEL FRAME WITH STEEL-CONCRETE COMPOSITE BEAM UNDER CYCLIC HORIZONTAL LOADING

by M.Yamada[I], B.Tsuji[II] and H.Adachi[III]

SUMMARY

In order to clarify the elasto-plastic behavior of steel frames with steel-concrete composite beam under the seismic force, cyclic horizontal loading tests are performed. The specimens are the rectangular steel unit rigid frame with reinforced concrete slabs having four kinds of thickness. Deformation analysis is carried out using the points model as the cross section and an isotropic-kinematic hardening model as the behavior of the steel. Considering the shear lag of the concrete slab, in-plane shear crack analysis is performed. Agreement between the analysis and the experiment is fairly well. Relationship between the slab thickness and the failure mode of the composite beam is discussed.

INTRODUCTION

Steel frames with the steel-concrete composite beams are often used in building structures. However, few tests have been performed to investigate the elasto-plastic behavior of the composite beam under alternately repeated cyclic loading [1,2]. The objective of the present study is to investigate the elasto-plastic and collapse behavior of the steel unit rigid frame with the composite beams having various concrete slab thicknesses such as shown in Figs.1 and 2. Monotonous loading and incremental horizontal sway deflection amplitude cyclic loading tests are carried out until the fracture at some part of the frame occurs. Elasto-plastic analysis is carried out considering the shear lag of the concrete slab and the cyclic hardening and the Bauschinger's effects of the steel. In-plane shear crack of the concrete slab is analyzed using an elliptic fracture criteria under the combined axial and shearing stresses. Analytical results are compared with the test results.

ANALYSIS

Elasto-plastic deformation behavior of the frame such as shown in Fig.1 is analyzed under the following assumptions. The wide flange steel beam and column cross sections are simplified into equivalent three points model [3], and the reinforced concrete slab into seven points model such as shown in Fgi.3. Tri-linear type cyclic stress-strain relationship of the mild steel is obtained from the series model of the isotropic-kinematic hardening material [4] such as shown in Fig.4. Material behavior of each element is also shown in Fig.4. Fig.5 shows the behavior of the series model considering the cyclic hardening effect and the Bauschinger's effect. The compressive stress-strain relationship of the concrete is negative bi-linear type such as shown in Fig.6. Each beam and column is divided into six line elements. The cubic and linear equations are assumed as

I Prof. Dr-Ing., Faculty of Engrg., Kobe Univ., Kobe, Japan.
II Assist. Prof., Faculty of Engrg., Kobe Univ., Kobe, Japan.
III Structural Engr., Tokai Kogyo Co., Osaka, Japan.

the incremental displacement functions for the lateral and axial directions. Considering the experimentally obtained parabolic axial strain distribution of the concrete slab in the transverse direction, such as shown in Fig.15, the strain distribution of the seven points model is assumed as is shown in Fig.7. Second order numerical analysis is performed. Lateral load-deformation relationships obtained are shown in Figs.11 and 12 by the broken line. In the small deflection range, the loop is spindle shape. As the deflection increses, the loop shows some slip phenomenon due to the tensile crack of the concrete slab.

In-plane shear crack of the concrete slab is also analyzed using the elliptic fracture criteria under the combined stresses [5]. The shearing stress τ at the root of the concrete slab is obtained by the following equation.

$$\tau(z,0)=\int_0^a \sigma(z,x)tdx-\int_0^a \sigma(z+dz,x)tdx/tdz \qquad \cdots\cdots (1)$$

where $\sigma(z,x)$ is the compressive stress shown in Fig.8, 't' the thickness of the slab and 'a' the width of the slab. The elliptic fracture criteria shown in Fig.9 is

$$\tau_F/F_C=\sqrt{-0.1(\sigma_F/F_C)^2+0.09(\sigma_F/F_C)+0.01} \qquad \cdots\cdots (2)$$

where (σ_F,τ_F) is the combination of the critical axial and shearing stresses and F_C is the compressive strength of the concrete cylinder. When the combination of the axial stress and the shearing stress at some part of the concrete slab reaches the critical condition, the in-plane shear crack appears. After the appearance of the shear crack, the shearing stress is assumed to be transmitted by the transverse reinforcement. The direction θ of the shear crack shown in Fig.8 is obtained by the following equation.

$$2\theta=\tan^{-1}(2\tau_F/\sigma_F) \qquad \cdots\cdots (3)$$

Analytical result of in-plane shear crack distribution by the fifth cycle is shown in Fig.16. Shear crack increses as the thickness of the slab decreases.

EXPERIMENT

The specimen tested is shown in Fig.1. The steel unit rigid frame is made of rolled wide flange profile. The main- and sub-beams are welded to the column. The panel zone at the beam-to-column joint is strengthened by the diagonal stiffner. Because of symmetry, the reinforced concrete slabs are connected at the top flange of the lower beam and at the bottom flange of the upper beam. The stud shear connector of 6 mm diameter is used. Sufficient number of stud connectors are used for the perfect rigid connection between the steel beam and the concrete slab. Four kinds of reinforced concrete slab thickness are employed such as shown in Fig.2. Longitudinal and transverse reinforcements are the same for all specimens. Material properties of the steel and the concrete used are shown in Table 1.

Loading system is shown in Fig.10. The test specimen is set in the loading frame with pin-roller supports. The constant vertical load of the column ($N=1/3N_y$) is applied by the testing machine. The lateral load is applied diagonally by the oil jack with load cell. Monotonous lateral load is applied only for the specimen C1 (slab thickness t=35 mm), and the result is compared with the behavior of the steel frame without

concrete slab. Alternately repeated cyclic loadings are applied with incremental horizontal sway deflection amplitudes. Increment of the sway rotation angle in each cycle is 1/200. Deflections of the beam and the column are measured by the dial gages and the strain distributions by the Fritz Staeger contact type strain gage and the electrical resistance gages.

EXPERIMENTAL RESULTS AND DISCUSSIONS

The load-deflection curves obtained are shown in Figs.11 and 12. The solid line shows the experimental result and the broken line the analytical one. The dot-dash line in Fig.11 shows the behavior of the steel frame without the concrete slab. Difference between the solid line and the dot-dash line shows the effect of the composite action of the concrete slab. For the specimen without concrete slab, lateral buckling of the beam occurs in the plastic range. Fig.12 shows the load-deflection relationship under the alternately repeated cyclic loading. The tensile crack of the concrete slab appears at the first cycle for all specimens. Before the maximum load is attained, the load-deflection curves of four specimens show nearly the same behavior, irrespective of the difference of the thickness of the concrete slab. Agreement between the experimental and the analytical results is fairly well in this range.

Cyclic loadings are continued until the fracture at some part of the specimen occurs. Two types of the fracture mode are observed. For the specimens C4 and C5, having relatively thin concrete slab (t=20 and 25 mm), in-plane shear cracks appear and spread along the flange tip of the steel beam and also along the slab haunch. These cracks pass through the whole length of the concrete slab and separation between the concrete slab and the steel beam occurs at the sixth cycle. And lateral buckling of the steel beam occurs due to the release of the lateral support by the concrete slab. Finally, crack at the welded beam-to-column joint occurs. For the specimens C2 and C3, having relatively thick concrete slab (t=30 and 35 mm), in-plane shear crack appears at the root of the concrete slab at the fourth cycle. These cracks spread along the root of the slab gradually as the deflection amplitude increses, but the separation between the concrete slab and the steel beam does not occur. At the eighth or ninth cycle, the crack at the welded beam-to-column joint occurs, and these specimens fail by the spreading of this crack.

Fig.13 shows the deflection curve of the composite beam at the maximum sway deflection of each cycle. After the tensile crack of the concrete slab occurs, the deflection at the positive bending moment region becomes smaller than at the negative bending moment region due to the composite action of the concrete slab. For the composite beams with thin concrete slab (t=20 and 25 mm), the deflection at the positive bending moment region increases after the in-plane shear crack passes through the whole length of the root of the slab. This shows that the spreading of the in-plane shear crack decreases the composite action of the concrete slab.

Fig.15 shows the axial strain distribution of the concrete slab of the C3 specimen obtained by the Fritz Staeger contact type strain gage. The location at which the strain distribution measured is shown in Fig.1. The axial strain distributes parabolically both under positive and negative bending moments. From these results, effective width of the compressive slab is obtained. Fig.14 shows the variation of the effective width λ with the deflection amplitudes. Effective width decreases as the sway

deflection increases.

Considering these parabolic axial strain distributions of the concrete slab and using elliptic fracture criteria under the combined axial and shearing stresses, in-plane shear crack distribution is analyzed. Analyzed crack distribution at the fifth cycle is shown in Fig.16. The crack decreases as the thickness of the concrete slab increases. Fig.17 shows the experimentally obtained crack distribution of the upper slab. The thick line shows the in-plane shear cracks that have occured by the fifth cycle. Analytical crack distribution corresponds with the experimental result for the most part in this range.

CONCLUSIONS

Monotonous and incremental sway deflection amplitude cyclic loading tests are conducted to investigate the elasto-plastic deformation behavior and the collapse mechanism of the steel frame having the steel-concrete composite beam such as shown in Fig.1. Test results are compared with the analytical results.

Elasto-plastic deformation behavior analyzed considering the shear lag of the concrete slab and the cyclic hardening and the Bauschinger's effects of the steel coinsides fairly well with the experimental results. Before the maximum load is attained, the load-deflection curves of four specimens show nearly the same behavior although the thickness of the concrete slab differs with each other.

In-plane shear crack of the concrete slab analyzed using elliptic fracture criteria and parabolic axial strain distribution of the concrete slab corresponds well with the experimental results. In-plane shear crack decreases as the thickness of the concrete slab increases.

Two types of the fracture mode are observed. For the composite beam having relatively thin concrete slab, in-plane shear crack spreads along the root of the concrete slab and separation between the concrete slab and the steel beam occurs. For the composite beam having relatively thick concrete slab, crack at the welded beam-to-column joint occurs. This crack spreads from the flange to the web of the steel beam.

Restraining effect of the concrete slab on the lateral buckling of the steel beam is sufficient until the separation between the concrete slab and the steel beam occurs.

BIBLIOGRAPHY

1. Hisatoku,T. and Kato,Y. : The Experimental Studies on the Composite Beams, - Composite Steel-Concrete Beams with Welded Stud Shear Connection -, Takenaka Technical Research Report, No.7, 1971, pp.85/103, (in Japanese).
2. Humer,J.L. : Composite Beams under Cyclic Loading, Proc. ASCE, Vol.105, ST10, Oct., 1979, pp.1949/1965.
3. Yamada,M. and Shirakawa,K. : Elasto-Plastische Biegeformänderungen von Stahlstützen mit I-Querschnitt, Teil II : Wechselseitig wiederholte Biegung unter konstanter Normalkrafteinwirkung, Der Stahlbau, 40. Jahrg., H.3, 1971, S.65/74, u. H.5, 1971, S.143/151.
4. Yamada,M. and Tsuji,B. : Generalized Stress-Strain Relationship of Structural Steel, Part I : Isotropic-Kinematic Hardening Model, Trans. AIJ, Vol.270, Aug., 1978, pp.17/22, (in Japanese).

5.Yamada,M. and Tada,K. : Experimental Investigation on the Fracture Criteria of Concrete under Combined Stresses, RILEM Symposium, Cannes, Oct., 1972, Vol.1, pp.245/255.
6.Yamada,M., Tsuji,B. and Murazumi,Y. : Elasto-Plasitc Cyclic Horizontal Sway Behavior of Wide Flange Unit Rigid Frames Subjected to Constant Vertical Loads, IABSE Symp., Lisboa, Sep., 1973, pp.151/156.

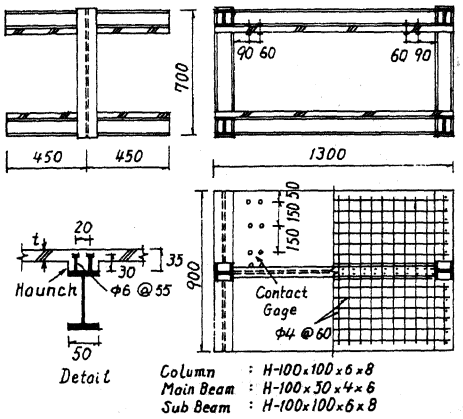

Fig.1 Test Specimen

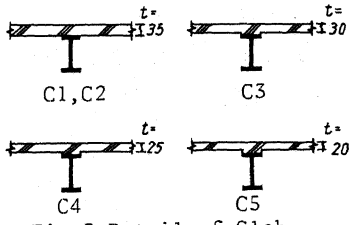

Fig.2 Detail of Slab

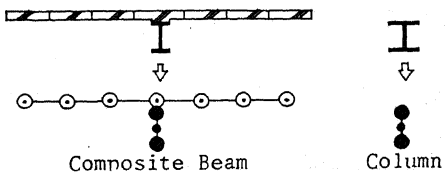

Fig.3 Points Model

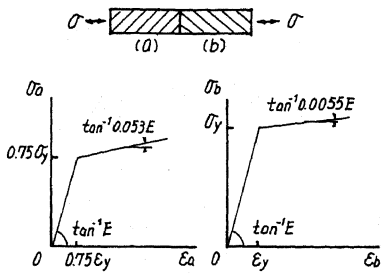

Fig.4 Series Model

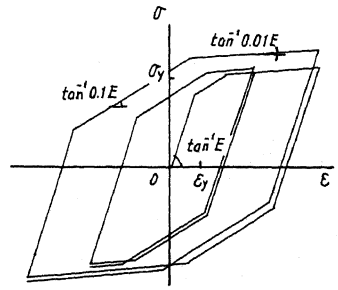

Fig.5 σ-ε Relation of Steel

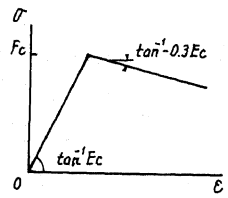

Fig.6 σ-ε Relation of Concrete

Table 1 Mechanical Properties

(a) Concrete

Specimen	C1	C2	C3	C4	C5
F_c(kgf/cm^2)	395	351	314	302	309
f_t(kgf/cm^2)	32	29	22	20	22

(b) Steel

	Column		Beam		Reinforce-ment
	Flange	Web	Flange	Web	
σ_y(tf/mm^2)	28.1	32.0	36.0	38.4	25.3

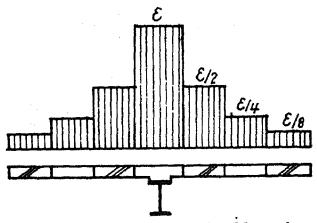

Fig.7 Strain Distribution of Slab

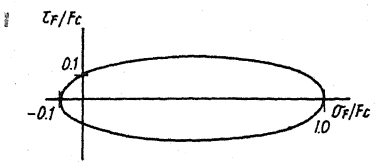

Fig.9 Fracture Criteria of Concrete

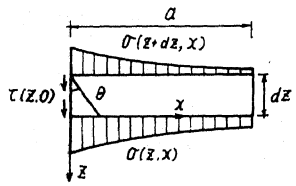

Fig.8 Stress Distribution of Slab

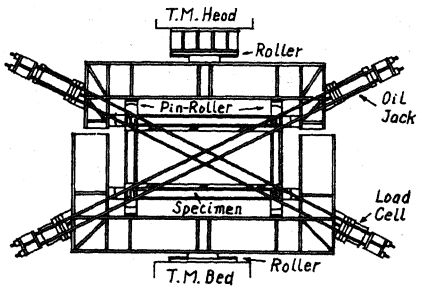

Fig.10 Loading System

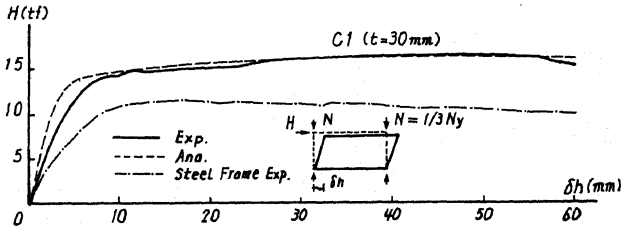

Fig.11 Load-Deflection Relationship

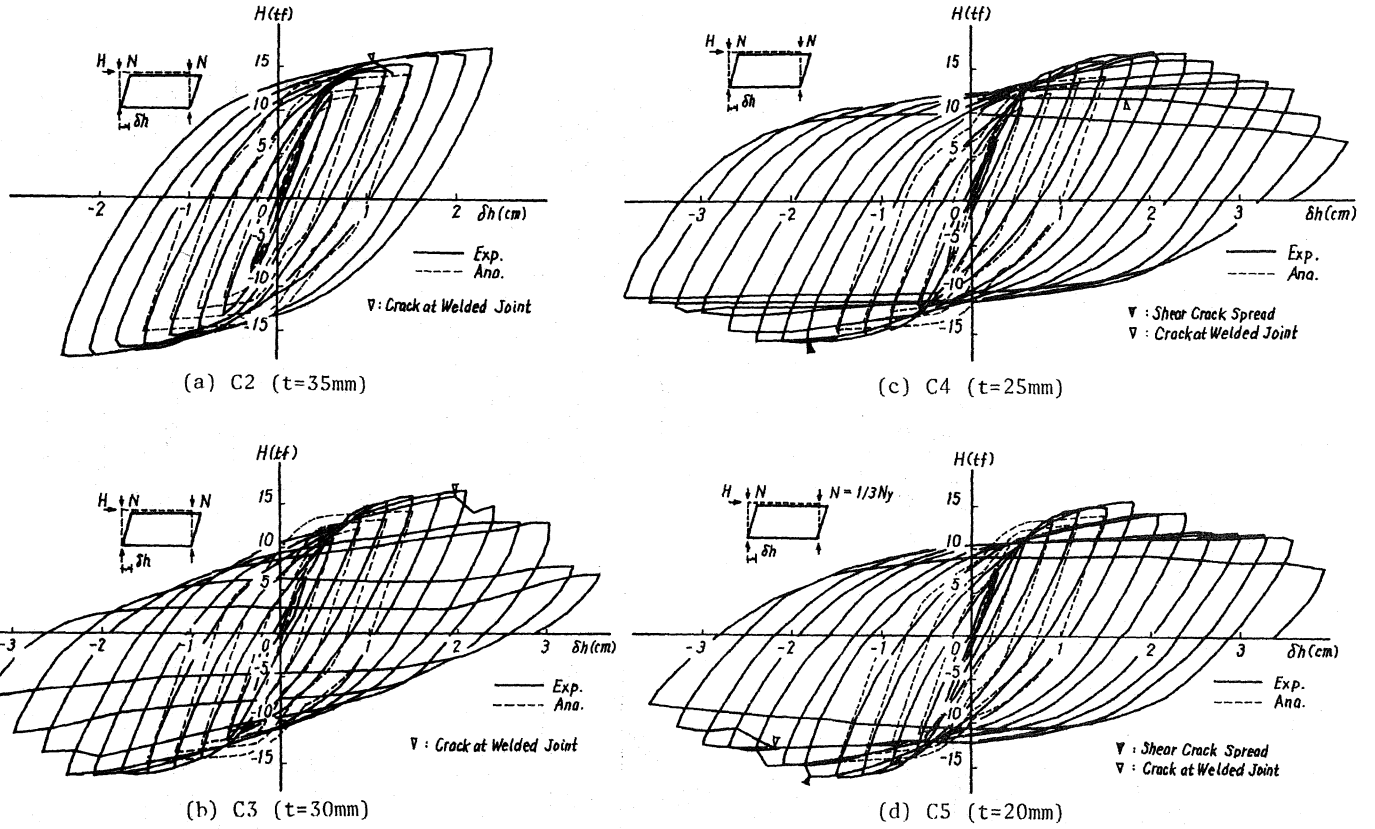

(a) C2 (t=35mm)

(c) C4 (t=25mm)

(b) C3 (t=30mm)

(d) C5 (t=20mm)

Fig.12 Load-Deflection Relationship

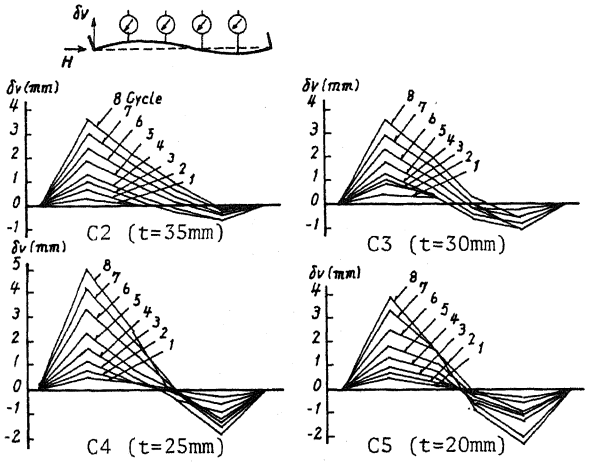

Fig.13 Deflection of Composite Beam

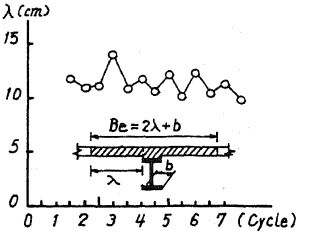

Fig.14 Effective Width

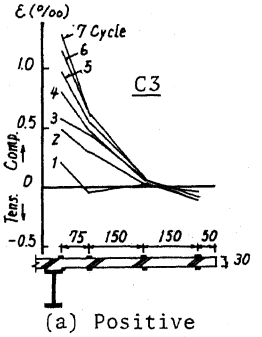

(a) Positive Moment

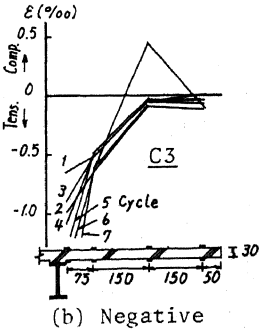

(b) Negative Moment

Fig.15 Strain Distribution

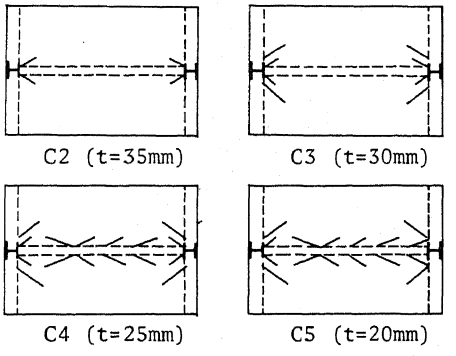

Fig.16 In-Plane Shear Crack

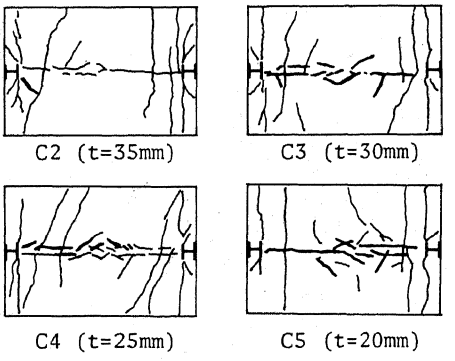

Fig.17 In-Plane Shear Crack